Arsenault JT, Rima S, Stemmann H, Vanduffel W. Role of the Primate Ventral Tegmental Area in Reinforcement and Motivation. *Current Biology* 2014, 24(12), 1347-1353.

Current Biology 24, 1347–1353, June 16, 2014 ©2014 Elsevier Ltd All rights reserved http://dx.doi.org/10.1016/j.cub.2014.04.044

Report

Role of the Primate Ventral Tegmental Area in Reinforcement and Motivation

John T. Arsenault,[1,2] Samy Rima,[1] Heiko Stemmann,[1] and Wim Vanduffel[1,2,3,*]
[1]Laboratory for Neuro- and Psychophysiology, KU Leuven, 3000 Leuven, Belgium
[2]Athinoula A. Martinos Center for Biomedical Imaging, MGH, Charlestown, MA 02129, USA
[3]Department of Radiology, Harvard Medical School, Boston, MA 02115, USA

Summary

Monkey electrophysiology [1, 2] suggests that the activity of the ventral tegmental area (VTA) helps regulate reinforcement learning and motivated behavior, in part by broadcasting prediction error signals throughout the reward system. However, electrophysiological studies do not allow causal inferences regarding the activity of VTA neurons with respect to these processes because they require artificial manipulation of neuronal firing. Rodent studies fulfilled this requirement by demonstrating that electrical and optogenetic VTA stimulation can induce learning and modulate downstream structures [3–7]. Still, the primate dopamine system has diverged significantly from that of rodents, exhibiting greatly expanded and uniquely distributed cortical and subcortical innervation patterns [8]. Here, we bridge the gap between rodent perturbation studies and monkey electrophysiology using chronic electrical microstimulation of macaque VTA (VTA-EM). VTA-EM was found to reinforce cue selection in an operant task and to motivate future cue selection using a Pavlovian paradigm. Moreover, by combining VTA-EM with concurrent fMRI, we demonstrated that VTA-EM increased fMRI activity throughout most of the dopaminergic reward system. These results establish a causative role for primate VTA in regulating stimulus-specific reinforcement and motivation as well as in modulating activity throughout the reward system.

Results

VTA-EM Reinforces Operant Behavior

Experiment 1

The firing pattern of ventral tegmental area (VTA) neurons is consistent with their putative function in reinforcement learning and motivational behavior [1, 2, 9]. Establishing a causal role for the primate VTA in such processes, however, has been hampered by a lack of targeted focal perturbation studies. We therefore developed an MRI-guided method to perform chronic electrical microstimulation of VTA (VTA-EM) in nonhuman primates (see Supplemental Experimental Procedures available online). We used perioperative high-resolution imaging (Figure 1A; Movie S1) to direct the insertion of a guide tube and a microwire electrode array [10] and to confirm the final positioning of the electrodes (Figure 1B). After electrode implantation, we tested whether VTA-EM played a causal role in positive reinforcement by using an operant conditioning paradigm. All procedures were approved by the KU Leuven Committee on Animal Care and are in accordance with NIH and European guidelines for the care and use of laboratory animals.

Monkeys first performed a baseline cue preference test measuring their preferences between two simultaneously presented visual cues in a free-choice task. In each session, a new set of cues was used. Individual trials began with a randomized wait period (1,000–1,500 ms) during which the monkey was required to fixate on a centrally positioned white square. After this, the white square was removed, and two visual cues appeared simultaneously on the left and on the right side of the screen (Figure 2A). Monkeys were allowed to freely select one of the two cues by saccading to their choice. To motivate cue selection, we rewarded 50% of all saccades with juice (0.07 ml). Critically, juice reward probabilities were equalized across cue positions (left or right) and cue identity (cue A or cue B) and, hence, were completely independent of the monkey's choice (see Supplemental Experimental Procedures).

For consistency across sessions, the preferred and nonpreferred cues during the baseline test were deemed cue A and B, respectively. After the baseline preference test was completed, we began a cue B-*VTA-EM* block in which 50% of all cue B selections were followed by VTA-EM. VTA-EM consisted of a 200 ms train of bipolar stimulation pulses (200 Hz; 650 μA–1 mA; two VTA electrodes; electrical microstimulation [EM] parameters, except the current, were identical for experiments 1–3). Importantly, to determine whether VTA-EM reinforced preceding actions, we performed VTA-EM 32–48 ms after cue selection (Figure 2B). Juice rewards were given in 50% of the trials but were entirely independent of VTA-EM, cue identity, and cue position. After the cue B-*VTA-EM* block, we began pairing VTA-EM with cue A selections (by using the paradigm explained above) and stopped pairing VTA-EM with cue B selections (cue A-*VTA-EM* block).

To quantify the monkey's cue selection behavior, we calculated a cue preference index: ([cue B selections − cue A selections]/[cue B selections + cue A selections]). This index ranges from 1 to −1, indicating a total preference for cue B or A, respectively. Cue preference indices taken from example sessions of monkey 1 (M1) and M3 (Figures 2C and 2D) provide clear evidence that the subject's preference for the cue associated with VTA-EM increased during the cue-*VTA-EM* blocks. Furthermore, these data indicate that the shift in cue preference was largest during the later stages of an EM block, as expected after repeated reinforcement. To quantify these effects, we split the data into the first and second half of each block (baseline, cue A- and cue B-*VTA-EM*) and calculated the mean cue preference during each half block. Because the effect of VTA-EM on cue preference was most evident during the second half of EM blocks (i.e., after the value of both cues could be sampled repeatedly), the mean cue preference during the second half of each block was compared across sessions. The mean cue preference of both M1 and M3 (Figures S1A and S1C) showed a main effect of block (Friedman test, $p < 0.05$). Comparison of the mean cue preference during the second half of blocks from M1 and M3

*Correspondence: wim@nmr.mgh.harvard.edu

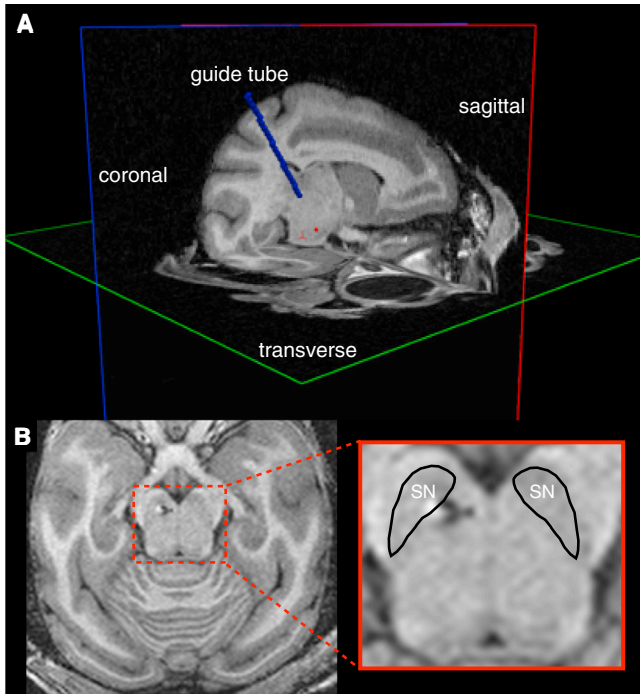

Figure 1. MRI-Guided Guide Tube and Electrode Implantation

(A) Triplanar cross-section of T1-weighted anatomical image acquired during guide tube insertion. Hypointensity induced by guide tube (see Movie S1) was used to estimate guide tube trajectory and position during surgery (blue cylinder). Estimated VTA target projected from the trajectory of the guide tube (red sphere).

(B) Postoperative T1-weighted anatomical image used to confirm the final electrode position. This transverse slice was the most ventral to exhibit hypointensity from the electrode. The inset displays an expanded view of the midbrain and electrode with the substantia nigra [SN] outlined.

See also Movie S1.

demonstrates the consistency of the VTA-EM effect across sessions (Figures 2E and 2F). Next, we hypothesized that the preference for the VTA-EM-associated cue should increase as a function of time within an EM block because positive feedback should occur between VTA-EM reinforcement and increased cue selection. Therefore, we calculated the correlation between elapsed time within a cue-VTA-EM block and preference for the cue associated with VTA-EM. Both M1 (mean r = 0.55, SEM r = 0.15, p = 0.03) and M3 (mean r = 0.47, SEM r = 0.06, $p = 6.59 \times 10^{-6}$) exhibited a significant positive correlation (sign-rank test, $p < 0.05$) across blocks, confirming the hypothesis that cue preference increases as a function of time (Figures S1B and S1D).

In an effort to better understand the effect of juice and VTA-EM reinforcement on trial-by-trial cue selection behavior, we utilized Kalman filter learning models (http://www.cs.bris.ac.uk/home/rafal/rltoolbox/; see Supplemental Experimental Procedures) [11, 12]. For each monkey, two separate learning models were generated. One model used juice administration as the reward input, whereas the other model used VTA-EM. The other parameters of the model were assumed to be free. These free parameters were then fit to each subject's trial-by-trial cue selection behavior in order to maximize the likelihood of explaining the animal's observed behavior (Table S1). We found that the models utilizing VTA-EM as the reward input provided a better fit for the cue selection behavior (see Akaike information criterion [AIC] calculation in Supplemental Experimental Procedures) of both M1 ($\Delta AIC = 9.6$, $AIC_{weight} = 121.5$) and M3 ($\Delta AIC = 152.6$, $AIC_{weight} = 1.37 \times 10^{33}$). Thus, VTA-EM reinforcement explains trial-by-trial cue selection behavior better than juice administration, despite the same frequency of juice and VTA-EM events following the VTA-EM-associated cue. The better fit of VTA-EM reinforcement likely results from transition periods when the relative frequency of reinforcement events are exactly balanced between cues for juice, but not VTA-EM, predicting the subsequent shift in cue preference. We next examined the SD of the diffusion (σ_d) parameter to infer learning rates because larger σ_d values lead to higher learning rates. Juice models for M1 and M3 were found to display higher σ_d values. This indicates that cue selection was more sensitive to juice administration in recent trials, whereas reinforcement from VTA-EM events was integrated over longer periods of time. Next, the exploration (i.e., inverse temperature) parameter was compared between the two reinforcers because higher values indicate less-noisy selections (i.e., more-frequent selection of the high-value cue as calculated by the model). The larger exploration parameter of the VTA-EM models for both M1 and M3 therefore indicated that cue selection behavior was less noisy when VTA-EM reinforcement was modeled. Thus, the Kalman filter learning models confirmed in both animals that VTA-EM reinforcement better accounted for trial-by-trial cue selection behavior while indicating that VTA-EM reinforcement was integrated over longer time periods and was used to exploit the high-value cue more often, relative to equiprobable juice reinforcement.

Pavlovian Cue-VTA-EM Associations Motivate Future Cue Selection

Experiment 2

We developed a paradigm to assess whether Pavlovian cue-*VTA-EM* associations would motivate cue selection during a subsequent instrumental task. Importantly, within this paradigm there was no direct relationship between actions and VTA-EM during the association block or between the cue and VTA-EM during the instrumental block. Therefore, this paradigm offers insight into the motivational function of VTA-EM because it assesses whether a cue acquires incentive motivation during a Pavlovian association [13, 14]. This paradigm began with a 400-trial baseline cue preference test identical to the baseline test performed in experiment 1 in the absence of VTA-EM (Figure 3A). After this test, the subject was exposed to a 20 min Pavlovian cue-*VTA-EM* association block. Within this block, the subject performed a passive fixation task to obtain a juice reward (0.03 ml) every 800–1,200 ms while every 3,500–6,000 ms, one of the two visual cues was randomly presented. VTA-EM occurred 400 ms into every 500 ms presentation of the initially nonpreferred cue B. During this block, cue A was presented as often as cue B but never coupled with VTA-EM. After this Pavlovian association block, an identical 400-trial cue preference test was performed. If animal performance permitted, we performed another 20 min Pavlovian association block in which the VTA-EM-coupled cue was switched to cue A. This was followed by another 400-trial cue preference test block.

Cue preference indices from example sessions in M2 (Figure 3B) and M3 (Figure 3C) demonstrate an increased preference for cue B following the cue B-VTA-EM Pavlovian association block. After the subsequent cue A-VTA-EM association block, there was another shift in cue preference toward the cue previously associated with VTA-EM. To quantify the effect

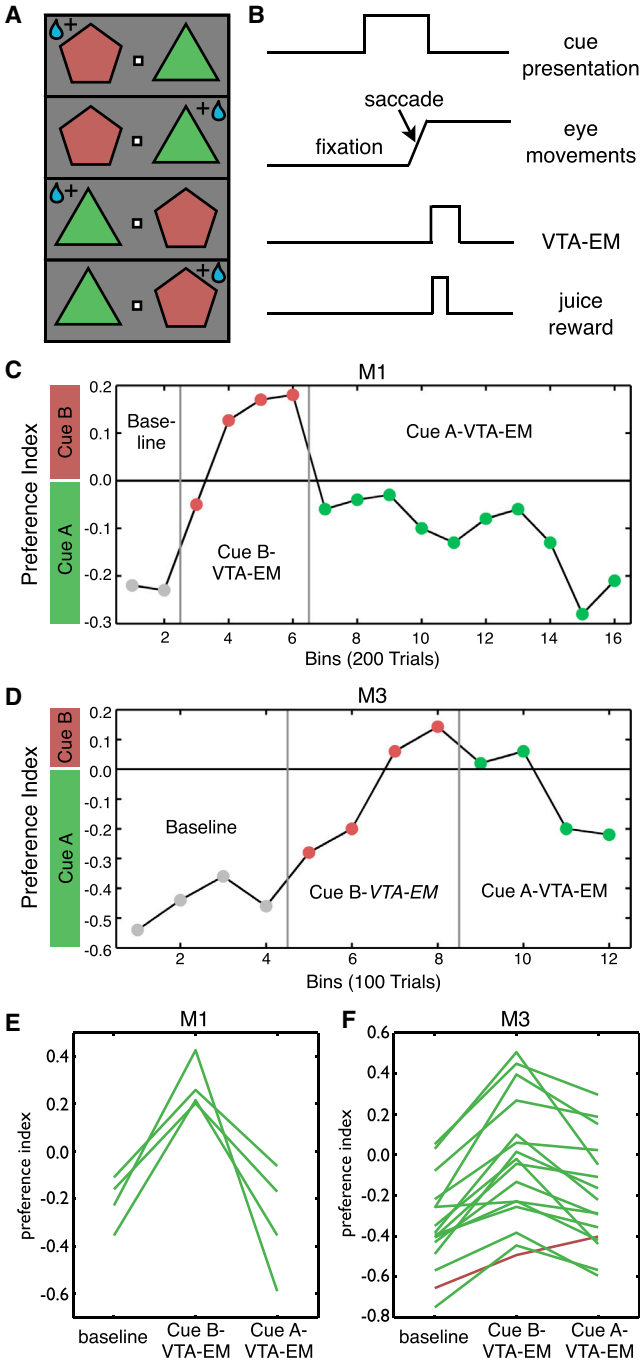

Figure 2. VTA-EM Reinforces Cue Selection in Experiment 1

(A) Four pseudorandomized, equiprobable trial types used in the free-choice visual cue preference test. New pairs of cues were used in each session. Juice reward probability was equalized across cue position and cue identity.

(B) Timing schematic of cue presentation, eye movements, juice reward (100 ms, 50% of trials), and VTA-EM (200 ms, 50% of selections of VTA-associated cue during cue-*VTA-EM* blocks). Juice and VTA-EM occurred 32–48 ms after cue selection.

(C and D) Cue preference index ([cue B selections – cue A selections])/(cue B selections + cue A selections]) during a single-example session of the operant task for subjects M1 (C) and M3 (D). Cue preference index was calculated in bins of 100 and 200 trials for M1 and M3, respectively. Color of data points denotes the cue selection followed by VTA-EM on 50% of the trials (gray: no *VTA-EM*; red: cue B-*VTA-EM*; green: cue A-*VTA-EM*). VTA-EM consisted of a 200 ms train of bipolar stimulation pulses (200 Hz; 650 μA [M1], 1 mA [M3]; two VTA electrodes stimulated simultaneously).

of cue-*VTA-EM* associations on cue preference, the mean cue preference before an association block was compared to the mean cue preference after an association block. For consistency across these pairs of cue preference test blocks, the cue associated with VTA-EM during the intervening association block was designated cue B. We found that both M2 and M3 (Figures S2A and S2B) exhibited a significantly increased preference for cue B after cue B-VTA-EM (sign-rank test, $p < 0.05$). Examination of the mean cue preference between the two preference tests demonstrates the consistency of the VTA-EM effect in experiment 2 for M2 and M3 (Figures 3D and 3E). This cue-specific effect is comparable to specific Pavlovian instrumental transfer (PIT) [15–17] because both paradigms demonstrate that incentive motivation acquired through Pavlovian association can be selectively transferred to an instrumental task. Importantly, to encourage responses, from which cue-selective effects could be monitored, the postassociation instrumental task was performed with 50% juice reward probability and was not under extinction as is characteristic for traditional PIT paradigms. Thus, our paradigm was not well suited to examine the general form of PIT during which general increases in vigor are displayed [15–17]. Nonetheless, because subjects could respond immediately after visual cue presentation, we examined changes in reaction times (RT) as an indicator of vigor. No significant change in the RT (sign-rank test, $p > 0.25$) for preference tests performed before and after Pavlovian association blocks was found for both M2 ($n = 6$ pairs of blocks, $p = 1.00$) and M3 ($n = 28$ pairs of blocks, $p = 0.265$). In general, experiment 2 demonstrated that cue-VTA-EM associations allowed a cue to gain incentive motivation leading to its increased selection during a subsequent operant task.

VTA-EM Increases fMRI Activity in the Dopaminergic Reward Network

The dopaminergic reward network consists of structures that receive dense dopaminergic innervation and respond to reward-related tasks. Comparison of a meta-analysis of 142 human fMRI studies of reward processing [18] and primate dopamine receptor innervation [19, 20] reveals the nucleus accumbens (NA), caudate, putamen, thalamus, orbitofrontal cortex (OFC), anterior insula, anterior cingulate cortex (ACC), and prefrontal cortex (PFC) as major nodes in this network. In addition, the hippocampus and the amygdala also exhibit reward responses and strong dopaminergic connections [20]. Human fMRI studies have found that nodes within the dopaminergic reward network, such as the ventral striatum and OFC, exhibit modulations in functional activity that correlate with similar reward prediction error signals as coded by the phasic activity of dopamine neurons [21, 22]. This correlative evidence suggests that reward activity within these regions may be driven, in part, by phasic VTA responses. Nonetheless, the distributed network of structures modulated by phasic changes in VTA activity has not been causally investigated in primates. To do so, we utilized combined VTA-EM fMRI [23].

During the scanning procedure, juice rewards (0.03 ml) were administered every 800–1,200 ms to maintain fixation

(E and F) Mean cue preference indices during the second half of each block type for each full session performed by M1 (E) and M3 (F). Green lines denote a session with a consistent trend for increased preference for the cue reinforced with VTA-EM, whereas red lines represent the opposite trend.

See also Figure S1 and Table S1.

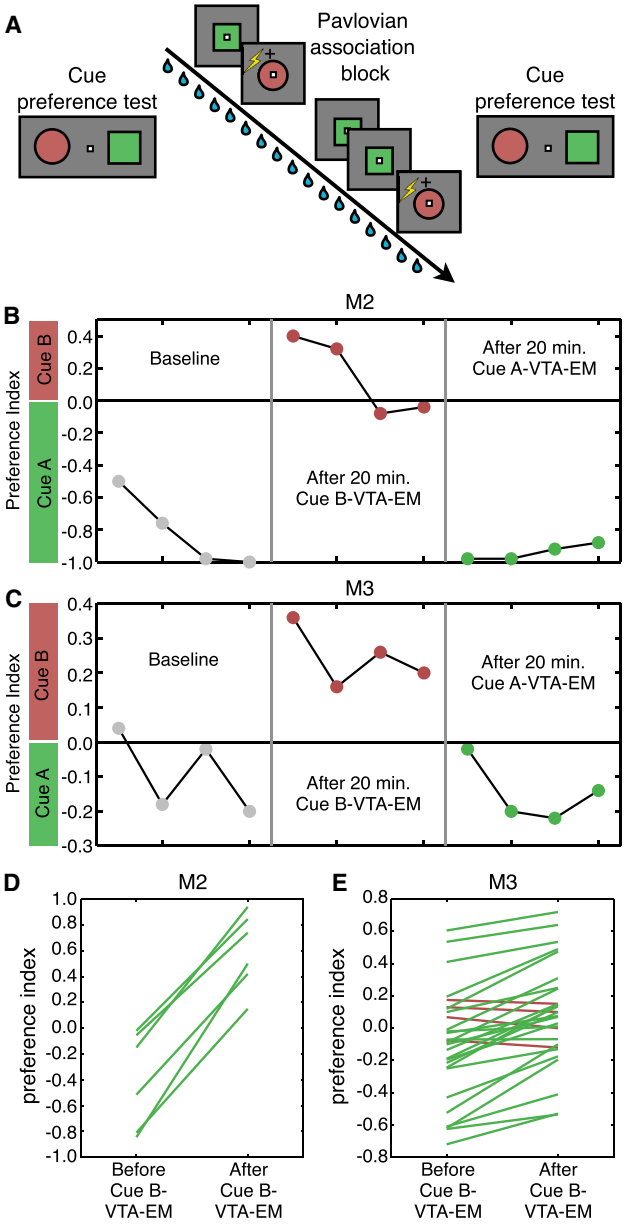

Figure 3. Pavlovian Cue-VTA-EM Association Motivates Future Cue Selection in Experiment 2

(A–C) Paradigm consisted of a 20 min Pavlovian cue-*VTA-EM* association block surrounded by two cue preference test blocks (no VTA-EM) (A). During the Pavlovian association block, the monkey performed a passive fixation task (0.03 ml of juice every 800–1,200 ms) while only one of the two visual cues (500 ms presentation) shown every 3,500–6,000 ms was temporally associated with VTA-EM (400 ms into cue presentation; bipolar; 200 ms; 200 Hz; 1 mA; two VTA electrodes stimulated simultaneously). The cue preference index from cue preference tests was calculated in bins of 100 trials from single-example sessions performed by M2 (B) and M3 (C). Color of data points denotes the preceding Pavlovian association block (gray: no VTA-EM; red: cue B-VTA-EM; green: cue A-VTA-EM).

(D and E) Mean cue preference index values for each pair of blocks performed by M2 (D) and M3 (E). Green lines denote pairs of cue preference test blocks with a trend for an increased preference of the cue associated with VTA-EM during the intervening Pavlovian association block, whereas red lines represent the opposite trend.

See also Figure S2.

behavior, whereas VTA-EM and control trials (no VTA-EM), used to assess the brain-wide functional effects of VTA-EM, occurred every 3,900–6,400 ms. To generate a representative map of the activations elicited by VTA-EM, fMRI data sets from each subject were first coregistered to the 112 RM-SL space [24]. A whole-brain, voxel-by-voxel general linear model analysis was then performed (see Supplemental Experimental Procedures). The resultant statistical image (VTA-EM − no VTA-EM, false discovery rate (FDR) corrected, p = 0.001, cluster size: 10 voxels) reveals a broad network of activated structures (Figure 4). To quantify the regions activated by VTA-EM, we determined the volume of overlap between a large group of anatomical regions of interest (ROIs) and activated voxels (Table S2A). Activations were found within many of the nodes of the dopaminergic reward network discussed above and were predominantly found ipsilateral to the site of VTA-EM. Interestingly, current levels used to robustly activate the dopaminergic reward network ($\leq$392 μA) were much weaker than those needed to reinforce behavior (>650 μA).

To more directly assess the correspondence between the regions activated by VTA-EM and those activated by a natural reinforcer, we compared VTA-EM-driven activity to fMRI activity generated by unexpected juice reward (see Supplemental Experimental Procedures). Because M1 and M2 were not available for further experiments, we made comparisons with a separate group of animals (see experiment 2 in [24]) Juice-driven activity was thresholded at the same level as VTA-EM in Figure 4 (juice − fixation, FDR corrected, p = 0.001, cluster size: 10 voxels), and a conjunction analysis was performed (Figure S3; see Supplemental Experimental Procedures). All anatomical ROIs displaying direct voxel-to-voxel colocalization of VTA-EM- and juice-driven activity are reported in Table S2B (highlighted in red). Several ROIs also displayed activations in response to both unexpected juice and VTA-EM but within nonoverlapping voxels (Tables S2A and S2C, highlighted in green). Despite this lack of an exact spatial correspondence at voxel level, this analysis demonstrates that the activation of these anatomical structures was common to both natural (unexpected juice) and artificial (VTA-EM) reinforcement. The majority of regions activated by both VTA-EM and juice (45B [PFC], areas 12 and 13 [OFC], area 24 [ACC], anterior intraparietal [AIP] area, caudate, gustatory, insula putamen, precentral opercular [PrCO], and ventral lateral nucleus [VL, thalamus]) were regions found in a meta-analysis of human reward studies [18] or were regions found to respond to primary reinforcers [25, 26]. This correspondence confirms that VTA-EM activates most of the structures typically activated by natural reinforcers. The other regions displaying juice and VTA-EM activations were mainly somatosensory and motor and/or premotor regions (areas 1 and 2, area 3a and 3b, frontal area 1 [F], F3, F5a, F5c, rostral inferior parietal lobule [PF], and secondary somatosensory cortex [SII]). Although activation of these structures in the juice experiment could result from the motor component of juice consumption, there were no differences in the juice administered temporally surrounding VTA-EM and the no VTA-EM events (see Supplemental Experimental Procedures). Interestingly, these regions receive dense dopaminergic innervation and are affected by dopaminergic modulation [27, 28]. Lastly, regions driven by juice, but not VTA-EM, were predominantly found within higher-order visual areas (dorsal visual area [V4D], inferior lateral intraparietal [LIPi], fundus of superior temporal [FST], lower superior temporal

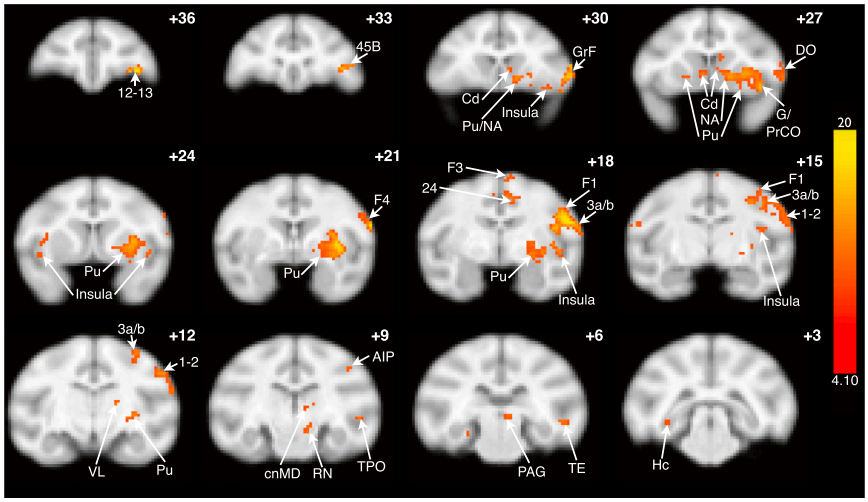

Figure 4. fMRI Activations Induced by VTA-EM in Experiment 3

Group analysis T score maps overlaid on coronal slices of the 112 RM-SL T1/T2* anatomical volume (n = 35 runs, M1 = 12 runs, M2 = 5 runs, M3 = 18 runs, fixed effect analysis, VTA-EM – no VTA-EM, FDR corrected, p = 0.001, cluster size: 10 voxels). VTA-EM consisted of a 200 ms train of bipolar stimulation pulses (200 Hz; 200 ms; 100 μA–392 μA; two VTA electrodes stimulated simultaneously).

The following abbreviations were used: AIP, anterior intraparietal; cnMD, centromedian nucleus; Cd, caudate; DO, dorsal opercular; G, gustatory; GrF, granular frontal; Hc, hippocampus; NA, nucleus accumbens; PAG, periaqueductal gray; Pu, putamen; PrCo, precentral opercular; RN, red nucleus; TPO, temporal parietal occipital; VL, ventral lateral nucleus.

See also Figure S3 and Table S2.

[LST], dorsal medial superior temporal [MSTd], middle temporal [MT], posterior inferior temporal cortex [TEO], anterior temporal cortex [TE], visual area 6 [V6], V6A, middle part of superior temporal polysensory [STPm]) (Table S2C). Activation of these regions in response to reward has been observed in previous monkey and human fMRI studies [29, 30]. This suggests that with the stimulation parameters utilized in this study, VTA-EM has little effect on higher-order visual regions. Lastly, the voxel-by-voxel analyses revealed that NA, a key node in the dopaminergic reinforcement network, was activated by VTA-EM, but not juice. In contrast, an ROI analysis of the anatomically defined NA revealed stronger activations by juice (n = 40 runs) than by VTA-EM (n = 35 runs) in left NA (VTA-EM mean percent signal change [PSC] = 0.09, juice mean PSC = 0.19, rank-sum test, p = 0.03) and right NA (VTA-EM mean PSC = 0.14, juice mean PSC = 0.24, rank-sum test, p = 0.007). This analysis suggests that juice reward increases fMRI activity more broadly throughout NA, whereas VTA-EM induced stronger yet more focal activations within NA. Despite the differences seen between activation maps generated by VTA-EM and unexpected juice reward, both reinforcers recruit a largely overlapping set of structures, many of them reward-processing structures with dense dopamine innervation.

Discussion

We have demonstrated that monkey VTA can be accurately and precisely targeted for chronic EM by using perioperative MRI guidance. VTA-EM was capable of selectively reinforcing and motivating behavior during operant and Pavlovian conditioning paradigms. This was demonstrated by an increased selection of a particular visual cue following the reinforcement of its selection with VTA-EM (experiment 1) or its previous Pavlovian coupling with VTA-EM (experiment 2). Therefore, this work establishes a causal role for primate VTA activity in the selective assignment of motivational value to visual cues, thus proving fundamental aspects of the hypothesized functional role of phasic neuronal VTA activity in primate behavior [1, 2, 13, 31]. Finally, by combining fMRI with simultaneous VTA-EM, we demonstrated that artificially increased VTA activity increased fMRI activity throughout most nodes of the dopaminergic reward network.

Comparison with VTA-EM and Optogenetic Stimulation in Rodents

Many rodent studies have demonstrated that VTA-EM [4, 7, 32], unaccompanied by other reinforcers, can reinforce operant behavior. In contrast, we monitored the behavioral effects of VTA-EM during tasks that were also reinforced with equiprobable juice reward. Juice rewards were employed because pilot experiments (M1, n = 10 sessions; M2 and M3, n = 1 session) demonstrated that VTA-EM alone, at least with the parameters utilized here, was not sufficient to maintain operant behavior. Consequently, balanced juice rewards were needed to maintain task performance, whereas unbalanced VTA-EM was used to affect cue preference. Therefore, although the VTA-EM-dependent effects on cue selection confirm VTA-EM's reinforcing properties, comparison with rodent results suggests that VTA-EM in rodents is a stronger reinforcer than VTA-EM in primates. Interestingly, operant reinforcement through optogenetic stimulation (OS) of dopamine neurons in rodents can also require the concurrent use of a primary reinforcer [3], but see [7, 32]. Because the majority of dopamine neurons phasically respond to unexpected reward [33], the typical motivational signal conveyed by the VTA to downstream structures likely involves VTA-wide activity. Therefore, a plausible interpretation of these results is that some OS paradigms in rodents (due to the smaller volume of tissue affected by OS [34]) and our EM paradigm in monkeys (due to the larger volume of VTA in primates) excite a smaller proportion of the total population of VTA neurons compared to rodent VTA-EM. Excitation of this smaller population may result in a weaker motivational signal and reduced behavioral effects. This is corroborated by our comparison of VTA-EM- and juice-induced fMRI activity within NA, which suggests that, in primates, natural reinforcers (juice) more broadly increase activity throughout reward structures. This may also explain why lower currents in the fMRI experiment were sufficient to drive the dopaminergic reward network, but higher currents were needed to reinforce behavior. In addition, an important caveat is that unlike the cell-type-specific OS now becoming common in rodent studies, VTA-EM likely stimulates dopaminergic (~65% of the population), GABAergic (~30%), and glutamatergic (~5%) cell types with little to no selectivity. Interestingly, OS of GABAergic VTA to NA projections has been shown to enhance stimulus-outcome associations [35]. Therefore, the

behavioral effect of VTA-EM's indiscriminate activation of VTA is likely a complex interaction of these different subpopulations and their targets. Despite this limitation, VTA-EM is an important first step in the causal understanding of VTA activity on motivation, reinforcement, and plasticity within the primate.

Comparison with Reinforcing Stimulation in Monkey

The primate exhibits greater dopamine innervation than the rodent. This expansion is evident in both densely (e.g., motor and premotor areas) and sparsely (i.e., parietal and temporal areas) innervated regions [8]. Furthermore, the laminar distribution of dopaminergic receptors differs between species, with layer 1 receiving the highest receptor density in primates while rodents display a more varied laminar distribution that is sparse in upper layers [8, 36]. These structural differences justify the importance of the primate model because they likely affect function. Nonetheless, the few studies assessing the reinforcing properties of EM in primate VTA or within a close proximity of VTA were large-scale mapping studies [37–39]. In these experiments, numerous locations were stimulated to determine reinforcing sites. The exact location of the EM sites was then determined using post hoc, ex vivo histology. Consequently, the behavioral experiments performed in these studies were conducted without precise knowledge of electrode positioning prohibiting a precisely targeted study of VTA function.

In addition, previous studies attempting to investigate the reinforcing effects of EM in VTA and neighboring structures have used a simple lever-pressing task. Although these studies demonstrated that EM reinforces operant behavior, they did not demonstrate the specificity of this reinforcement. For example, an important factor that governs Pavlovian and operant reinforcement is the temporal contiguity of the cue or the behavior and the reinforcement [40]. Because only one response was used in these earlier mapping studies, such studies cannot distinguish whether VTA-EM causes an aspecific increase in motivated behavior or whether it elicits effects that are specific to a particular cue or an action temporally associated with VTA-EM. In contrast, the changes in cue selection that we observed were dependent on temporal contiguity because increased cue selection was shown only for the cue whose presentation (Pavlovian) or selection (operant) was temporally coupled with VTA-EM. The specificity of this effect confirms that VTA-EM reinforcement selectively attributes motivational value to the cue temporally associated with VTA-EM. Moreover, the Pavlovian experiment demonstrates that VTA-EM can assign incentive motivation in a cue-selective way in the absence of any direct association with operant behavior.

In addition to VTA, EM has been shown to reinforce behavior at several other sites in the primate brain. These regions include NA, striatum, amygdala, OFC, lateral hypothalamus, mediodorsal nucleus, and locus coeruleus [38, 39, 41–43]. Interestingly, the majority of these sites contain a high density of dopamine receptors, and many of these same regions showed increased fMRI activity in response to VTA-EM and unexpected juice reward (see Figure 4 and Table S2). Moreover, it has been shown that systemic dopamine receptor blockade significantly reduced EM reinforcement within OFC, hypothalamus, and locus coeruleus [44]. Taken together, these findings suggest that these interconnected nodes of the dopaminergic reward network play important roles in reinforcement.

The absence over the last 40 years of any studies of primate VTA function causally linking activity with behavior and the complete absence of any previous work focusing specifically on VTA-EM highlight the difficulties of chronically targeting this small, but profoundly important, structure in primates. With the use of perioperative MRI-guided electrode implantation, we have circumvented these obstacles, allowing precise, chronic targeting of VTA. Furthermore, we have demonstrated the critical role of VTA in the selective reinforcement and motivation of visual cue selection. Finally, we combined fMRI with VTA-EM to demonstrate that VTA activity drives many of the nodes in the dopaminergic reward system. This work paves the way for future investigations of the relationship of increased VTA activity to reinforcement, motivation, learning, and plasticity throughout the primate brain.

Experimental Procedures

Please see Supplemental Experimental Procedures for a full description of the experimental design, methodology, and analysis.

Supplemental Information

Supplemental Information includes Supplemental Experimental Procedures, three figures, two tables, and one movie and can be found with this article online at http://dx.doi.org/10.1016/j.cub.2014.04.044.

Acknowledgments

We thank C. Klink, C. Fransen, C. Van Eupen, and A. Coeman for animal training and care; W. Depuydt, G. Meulemans, P. Kayenbergh, M. De Paep, S. Verstraeten, and I. Puttemans for technical assistance; and P. Balan and S. Raiguel for their valuable insights and comments on the manuscript. This work received support from Interuniversity Attraction Pole 7/21, Odysseus G.0007.12, Programme Financing PFV/10/008, Geconcerteerde Onderzoeks Actie 10/19, Impulsfinanciering Zware Apparatuur and Hercules funding of the KU Leuven, and Fonds Wetenschappelijk Onderzoek-Vlaanderen G090714N, G0888.13, G062208.10, G083111.10, G0719.12, and K7148.11. J.T.A. is a postdoctoral fellow of FWO-Vlaanderen. The Martinos Center for Biomedical Imaging is supported by National Center for Research Resources grant P41RR14075.

Received: June 25, 2013
Revised: March 27, 2014
Accepted: April 22, 2014
Published: May 29, 2014

References

1. Bromberg-Martin, E.S., Matsumoto, M., and Hikosaka, O. (2010). Dopamine in motivational control: rewarding, aversive, and alerting. Neuron *68*, 815–834.
2. Schultz, W., Dayan, P., and Montague, P.R. (1997). A neural substrate of prediction and reward. Science *275*, 1593–1599.
3. Adamantidis, A.R., Tsai, H.C., Boutrel, B., Zhang, F., Stuber, G.D., Budygin, E.A., Touriño, C., Bonci, A., Deisseroth, K., and de Lecea, L. (2011). Optogenetic interrogation of dopaminergic modulation of the multiple phases of reward-seeking behavior. J. Neurosci. *31*, 10829–10835.
4. Fibiger, H.C., LePiane, F.G., Jakubovic, A., and Phillips, A.G. (1987). The role of dopamine in intracranial self-stimulation of the ventral tegmental area. J. Neurosci. *7*, 3888–3896.
5. Tsai, H.C., Zhang, F., Adamantidis, A., Stuber, G.D., Bonci, A., de Lecea, L., and Deisseroth, K. (2009). Phasic firing in dopaminergic neurons is sufficient for behavioral conditioning. Science *324*, 1080–1084.
6. Esposito, R.U., Porrino, L.J., Seeger, T.F., Crane, A.M., Everist, H.D., and Pert, A. (1984). Changes in local cerebral glucose utilization during rewarding brain stimulation. Proc. Natl. Acad. Sci. USA *81*, 635–639.
7. Steinberg, E.E., Keiflin, R., Boivin, J.R., Witten, I.B., Deisseroth, K., and Janak, P.H. (2013). A causal link between prediction errors, dopamine neurons and learning. Nat. Neurosci. *16*, 966–973.

8. Berger, B., Gaspar, P., and Verney, C. (1991). Dopaminergic innervation of the cerebral cortex: unexpected differences between rodents and primates. Trends Neurosci. *14*, 21–27.
9. Roelfsema, P.R., van Ooyen, A., and Watanabe, T. (2010). Perceptual learning rules based on reinforcers and attention. Trends Cogn. Sci. *14*, 64–71.
10. Bondar, I.V., Leopold, D.A., Richmond, B.J., Victor, J.D., and Logothetis, N.K. (2009). Long-term stability of visual pattern selective responses of monkey temporal lobe neurons. PLoS ONE *4*, e8222.
11. Dayan, P., and Abbott, L.F. (2001). Theoretical Neuroscience: Computational and Mathematical Modeling of Neural Systems (Cambridge: MIT Press).
12. Daw, N.D., O'Doherty, J.P., Dayan, P., Seymour, B., and Dolan, R.J. (2006). Cortical substrates for exploratory decisions in humans. Nature *441*, 876–879.
13. Wassum, K.M., Ostlund, S.B., Loewinger, G.C., and Maidment, N.T. (2013). Phasic mesolimbic dopamine release tracks reward seeking during expression of pavlovian-to-instrumental transfer. Biol. Psychiatry *73*, 747–755.
14. Flagel, S.B., Clark, J.J., Robinson, T.E., Mayo, L., Czuj, A., Willuhn, I., Akers, C.A., Clinton, S.M., Phillips, P.E., and Akil, H. (2011). A selective role for dopamine in stimulus-reward learning. Nature *469*, 53–57.
15. Corbit, L.H., Janak, P.H., and Balleine, B.W. (2007). General and outcome-specific forms of Pavlovian-instrumental transfer: the effect of shifts in motivational state and inactivation of the ventral tegmental area. Eur. J. Neurosci. *26*, 3141–3149.
16. Corbit, L.H., and Balleine, B.W. (2011). The general and outcome-specific forms of Pavlovian-instrumental transfer are differentially mediated by the nucleus accumbens core and shell. J. Neurosci. *31*, 11786–11794.
17. Talmi, D., Seymour, B., Dayan, P., and Dolan, R.J. (2008). Human pavlovian-instrumental transfer. J. Neurosci. *28*, 360–368.
18. Liu, X., Hairston, J., Schrier, M., and Fan, J. (2011). Common and distinct networks underlying reward valence and processing stages: a meta-analysis of functional neuroimaging studies. Neurosci. Biobehav. Rev. *35*, 1219–1236.
19. Lidow, M.S. (1995). D1- and D2 dopaminergic receptors in the developing cerebral cortex of macaque monkey: a film autoradiographic study. Neuroscience *65*, 439–452.
20. Oades, R.D., and Halliday, G.M. (1987). Ventral tegmental (A10) system: neurobiology. 1. Anatomy and connectivity. Brain Res. *434*, 117–165.
21. Schonberg, T., O'Doherty, J.P., Joel, D., Inzelberg, R., Segev, Y., and Daw, N.D. (2010). Selective impairment of prediction error signaling in human dorsolateral but not ventral striatum in Parkinson's disease patients: evidence from a model-based fMRI study. Neuroimage *49*, 772–781.
22. O'Doherty, J.P., Dayan, P., Friston, K., Critchley, H., and Dolan, R.J. (2003). Temporal difference models and reward-related learning in the human brain. Neuron *38*, 329–337.
23. Ekstrom, L.B., Roelfsema, P.R., Arsenault, J.T., Bonmassar, G., and Vanduffel, W. (2008). Bottom-up dependent gating of frontal signals in early visual cortex. Science *321*, 414–417.
24. McLaren, D.G., Kosmatka, K.J., Oakes, T.R., Kroenke, C.D., Kohama, S.G., Matochik, J.A., Ingram, D.K., and Johnson, S.C. (2009). A population-average MRI-based atlas collection of the rhesus macaque. Neuroimage *45*, 52–59.
25. Scott, T.R., Yaxley, S., Sienkiewicz, Z.J., and Rolls, E.T. (1986). Gustatory responses in the frontal opercular cortex of the alert cynomolgus monkey. J. Neurophysiol. *56*, 876–890.
26. Rolls, E.T., Scott, T.R., Sienkiewicz, Z.J., and Yaxley, S. (1988). The responsiveness of neurones in the frontal opercular gustatory cortex of the macaque monkey is independent of hunger. J. Physiol. *397*, 1–12.
27. Hosp, J.A., Pekanovic, A., Rioult-Pedotti, M.S., and Luft, A.R. (2011). Dopaminergic projections from midbrain to primary motor cortex mediate motor skill learning. J. Neurosci. *31*, 2481–2487.
28. Pleger, B., Ruff, C.C., Blankenburg, F., Klöppel, S., Driver, J., and Dolan, R.J. (2009). Influence of dopaminergically mediated reward on somatosensory decision-making. PLoS Biol. *7*, e1000164.
29. Arsenault, J.T., Nelissen, K., Jarraya, B., and Vanduffel, W. (2013). Dopaminergic reward signals selectively decrease fMRI activity in primate visual cortex. Neuron *77*, 1174–1186.
30. Weil, R.S., Furl, N., Ruff, C.C., Symmonds, M., Flandin, G., Dolan, R.J., Driver, J., and Rees, G. (2010). Rewarding feedback after correct visual discriminations has both general and specific influences on visual cortex. J. Neurophysiol. *104*, 1746–1757.
31. Salamone, J.D., and Correa, M. (2012). The mysterious motivational functions of mesolimbic dopamine. Neuron *76*, 470–485.
32. Witten, I.B., Steinberg, E.E., Lee, S.Y., Davidson, T.J., Zalocusky, K.A., Brodsky, M., Yizhar, O., Cho, S.L., Gong, S., Ramakrishnan, C., et al. (2011). Recombinase-driver rat lines: tools, techniques, and optogenetic application to dopamine-mediated reinforcement. Neuron *72*, 721–733.
33. Mirenowicz, J., and Schultz, W. (1996). Preferential activation of midbrain dopamine neurons by appetitive rather than aversive stimuli. Nature *379*, 449–451.
34. Diester, I., Kaufman, M.T., Mogri, M., Pashaie, R., Goo, W., Yizhar, O., Ramakrishnan, C., Deisseroth, K., and Shenoy, K.V. (2011). An optogenetic toolbox designed for primates. Nat. Neurosci. *14*, 387–397.
35. Brown, M.T., Tan, K.R., O'Connor, E.C., Nikonenko, I., Muller, D., and Lüscher, C. (2012). Ventral tegmental area GABA projections pause accumbal cholinergic interneurons to enhance associative learning. Nature *492*, 452–456.
36. Lidow, M.S., Goldman-Rakic, P.S., Gallager, D.W., and Rakic, P. (1991). Distribution of dopaminergic receptors in the primate cerebral cortex: quantitative autoradiographic analysis using [3H]raclopride, [3H]spiperone and [3H]SCH23390. Neuroscience *40*, 657–671.
37. Plotnik, R., Mir, D., and Delgado, J.M.R. (1972). Map of reinforcing sites in the rhesus monkey brain. Int. J. Psychobiol. *2*, 1–21.
38. Briese, E., and Olds, J. (1964). Reinforcing Brain Stimulation and Memory in Monkeys. Exp. Neurol. *10*, 493–508.
39. Routtenberg, A., Gardner, E.L., and Huang, Y.H. (1971). Self-stimulation pathways in the monkey, Macaca mulatta. Exp. Neurol. *33*, 213–224.
40. Schultz, W. (2006). Behavioral theories and the neurophysiology of reward. Annu. Rev. Psychol. *57*, 87–115.
41. Rolls, E.T., Burton, M.J., and Mora, F. (1980). Neurophysiological analysis of brain-stimulation reward in the monkey. Brain Res. *194*, 339–357.
42. Mora, F., Avrith, D.B., and Rolls, E.T. (1980). An electrophysiological and behavioural study of self-stimulation in the orbitofrontal cortex of the rhesus monkey. Brain Res. Bull. *5*, 111–115.
43. Bichot, N.P., Heard, M.T., and Desimone, R. (2011). Stimulation of the nucleus accumbens as behavioral reward in awake behaving monkeys. J. Neurosci. Methods *199*, 265–272.
44. Mora, F., Rolls, E.T., Burton, M.J., Shaw, G.S., and Shaw, G.S. (1976). Effects of dopamine-receptor blockade on self-stimulation in the monkey. Pharmacol. Biochem. Behav. *4*, 211–216.